Graphene, its Homologues and Their Classification

L.B Drissi[a], E.H Saidi[a,b,c]

a. MAScIR-INANOTECH, Institute of Nanomaterials and Nanotechnology, Rabat, Morocco,

b. LPHE, Modelisation et Simulation, Faculté des Sciences Rabat, Morocco

c. Centre of Physcs and Mathematics, CPM-CNESTEN, Morocco

June 30, 2011

Abstract

Using tight binding model, lattice QFT and group theory methods, we study a class of lattice QFT models that are cousins of graphene; and which are classified by finite dimensional ADE Lie groups containing the usual crystallographic symmetries as discrete subgroups. We show in particular that the electronic properties of the 1D lattice poly-acetylene chain are given by a $SU(2)$ model and those of the well known 2D graphene by $SU(3)$. We also give two other models classified by $SU(4)$ and $SO(6)$ symmetries; they respectively describe 3D diamond and 3D lattice with octahedral sites. It is shown as well that the dispersion energies of this set of models are completely characterized by the roots of the Lie algebras underlying the symmetry groups. Other features, such as $SO(5)$ lattice involving sp^3d hybridization as well as the relation between the 4D hyperdiamond, having a $SU(5)$ symmetry and the 4D lattice QCD, are also discussed.

Keywords: Graphene, ADE Lie algebras, Tight binding model, Lattice QFT.

1 Introduction

Tight binding model is a simple lattice quantum field theory modeling the couplings between pairs of quantum states living at closed neighboring sites of the crystal [1, 2]. These short range pairings have been shown to describe quite adequately the electronic properties of graphene and homologues [3, 4, 5]. Tight binding approach is nicely represented in QFT in terms of hops of the delocalized electrons/holes from sites $\mathbf{r_n}$ of the crystal to nearest neighbors at $\mathbf{r_n} + \mathbf{v}_l$. These electron and hole hops will be interpreted

in this study in terms of step operators of Lie algebras that appear as hidden symmetries of lattices. This remarkable feature opens a window between continuous group representation theory, often used in elementary particles physics, and electronic properties in solid state physics involving representations of discrete symmetries [8]. As Lie groups are not common in solid state physics; we will refer below to these continuous groups as *hidden symmetries*; the well known crystallographic symmetries appear here as discrete subgroups of these continuous groups.

In this paper, we use tight binding method to engineer a series of *N- dimensional* lattice QFT models that are classified by ADE Lie groups of Cartan. In this modeling, the interactions between the first nearest neighbors are described by the basic representations of the leading elements of the Lie groups [9, 10, 11]. We show amongst others that the dispersion energies are completely determined by the root system of the underlying Lie algebras of these groups.

Our construction gives also a Lie group representation theory explanation of the idea of treating 2D honeycomb and higher dimensional homologue $\mathcal{L}$ as the superposition of two sublattices $\mathcal{A}$ and $\mathcal{B}$. At first sight the way of thinking about such lattices $\mathcal{L}$ as $\mathcal{A} \cup \mathcal{B}$ seems to be a beautiful trick; but it happens that it has a deep mathematical reason. In the case of $SU(N)$ models for instance, the two sublattices, denoted $\mathcal{A}_{SU(N)}$ and $\mathcal{B}_{SU(N)}$, are in fact intimately related with the *fundamental* $\underline{N}$ and *anti-fundamental* $\bar{N}$ representations of $SU(N)$ whose weight vectors $\boldsymbol{\mu}_l$ and $\boldsymbol{\mu}'_l$ satisfy the following constraint relations

$$
\begin{aligned}
\underline{N} &: \quad \boldsymbol{\mu}_1 + \boldsymbol{\mu}_2 + \ldots + \boldsymbol{\mu}_{N-1} + \boldsymbol{\mu}_0 &= 0 \\
\bar{N} &: \quad \boldsymbol{\mu}'_1 + \boldsymbol{\mu}'_2 + \ldots + \boldsymbol{\mu}'_{N-1} + \boldsymbol{\mu}'_0 &= 0
\end{aligned}
$$

which extend the well known one $\mathbf{v}_1 + \mathbf{v}_2 + \mathbf{v}_3 = \mathbf{0}$ of 2D graphene giving the *first nearest neighbors* and playing a central role in the study of electronic properties; in particular dispersion energy relation and the link with Dirac relativistic theory in 3D space time. The above constraint relations capture just the traceless condition of $SU(N)$; and have a physical interpretation in terms of conservation of total momenta.

Moreover, the *second nearest neighbors* of a lattice site at $\mathbf{r_n}$, and which contribute as first order corrections in the tight binding approach, are located at $\mathbf{r_n} + \mathbf{v}_{ij}$ with the $\mathbf{v}_{ij}$'s proportional to the vectors $\boldsymbol{\alpha}_{ij} = \boldsymbol{\mu}_i - \boldsymbol{\mu}_j$ which are exactly the $N(N-1)$ roots of $SU(N)$ symmetry; showing, amongst others, that the sublattices $\mathcal{A}_{SU(N)}$ and $\mathcal{B}_{SU(N)}$ has much to do with the root lattice of the $SU(N)$ group. In other words, sites $\mathbf{r_n}$ in the $\mathcal{A}_{SU(N)}$ and $\mathcal{B}_{SU(N)}$ sublattices of $\mathcal{L}_{SU(N)}$ are generated by simple roots like

$$
\mathbf{r_n} \quad \sim \quad n_1 \boldsymbol{\alpha}_1 + n_2 \boldsymbol{\alpha}_2 + \ldots + n_{N-1} \boldsymbol{\alpha}_{N-1} \tag{1.1}
$$

where the integral vector $\mathbf{r_n} = (n_1, n_2, \ldots n_{N-1})$ and where $\{\boldsymbol{\alpha}_1, \boldsymbol{\alpha}_2, \ldots, \boldsymbol{\alpha}_{N-1}\}$ are the *simple* roots of $SU(N)$.

Furthermore, by using known results on group theory methods in physics, the standard tight binding hamiltonian itself has as well a nice group theoretical interpretation; since the operators describing the electrons hops turn out to be nothing but step operators of the Lie algebra of $SU(N)$ symmetry. Within this view, one can use $SU(N)$ symmetry to build generalization of tight binding model that describe higher order couplings. In this regards, and though beyond the scope of this study, lessons learnt from *2D* conformal field theories show that one may borrow techniques from Kac-Moody algebras like Suggawara method [10] to extend standard tight binding method, describing pair couplings, to implement higher order interactions. In the present paper, we will mainly focus on exhibiting some basic features of the lattice $\mathcal{L}_{SU(N)}$ on which live the physics of the tight binding model. We also consider the example of $SO(6)$ model which has octahedral sites that form a vector representation of $SO(6)$.

To illustrate our idea, we study four examples of lattice models in diverse dimensions D; two of them, having respectively *D=1* and *D=2*, concern the electronic properties of the two following :

($\mathbf{1}$) the poly-acetylene chain [12] which, in our classification, turns out to correspond to a $SU(2)$ model. Here $SU(2)$ is the usual isospin group; it is the first element of the $SU(N)$ series with $N \geq 1$; its basic representation is the doublet with isospin states $| \pm \frac{1}{2} >$ satisfying the traceless property

$$s_z^{\uparrow} + s_z^{\downarrow} = \frac{1}{2} - \frac{1}{2} = 0.$$

($\mathbf{2}$) graphene, a sheet of graphite classified as a $SU(3)$ model. The basic representation of this group has three states with quantum numbers $\boldsymbol{\mu}_1$, $\boldsymbol{\mu}_2$, $\boldsymbol{\mu}_3$ (weight vectors in group theory language) that should be imagined as the extension of the weights $\pm\frac{1}{2}$ of $SU(2)$. These are *2D* vectors that satisfy the property

$$\boldsymbol{\mu}_1 + \boldsymbol{\mu}_2 + \boldsymbol{\mu}_3 = \mathbf{0}.$$

Two others *3D* lattice QFT systems given by the $SU(4)$ and $SO(6)$ models respectively based on tetrahedral (diamond) and octahedral crystals. To have delocalized electrons described by tight binding approach on these 3D lattices, one has to go beyond the usual sp^n hybridizations of carbon atoms; one needs for example material alloys with atoms having $sp^3 d^1$ ($sp^3 d^3$) hybridizations with delocalized electrons hoping to first nearest neighboring tetrahedral (octahedral) sites. But to illustrate the general idea in simple words, we consider rather two toy models for diamond and octahedron respectively based on the crystals $\mathcal{L}_{SU(4)}$ and $\mathcal{L}_{SO(6)}$ described in section 4 and 5.

The presentation is as follows: In section 2, we study the electronic properties of the ideal poly-acetylene chain. In section 3, we consider the case of graphene and show that it is precisely classified by the $SU(3)$ group. In section 4, we develop the $SU(4)$ diamond and in section 5, we study the octahedral model based on $SO(6)$. Last section is devoted to conclusion and comments.

2 Poly-acetylene chain as a $SU(2)$ model

Roughly, the poly-acetylene[1] chain is a linear molecule of carbon atoms in the sp^1 hybridization with delocalized electrons (2 pi-electrons per carbon atom). To study the electronic properties of this organic molecule, which in the present paper we take it in the ideal case; that is an infinite chain, we need to specify two main things:

- the 1-dimensional lattice of the carbon chain where live the delocalized electrons,

- the tight binding hamiltonian $\mathcal{H}_{SU(2)}$ describing the couplings between electrons belonging to closest neighboring atoms.

   the lattice
The *1D* lattice, denoted as $\mathcal{L}_{su(2)}$, is depicted in fig(1); it is isomorphic to the one-dimensional integer $\mathbb{Z}$- lattice with coordinates $x_m = md$ where d is the length of the carbon-carbon bond. There are two different, but equivalent ways, to deal with this lattice; one of them is that based on mimicking the study of the *2D* honeycomb of graphene; it is given by the superposition of two sublattices $\mathcal{A}_{su(2)}$ and $\mathcal{B}_{su(2)}$ (blue and red in the figure).
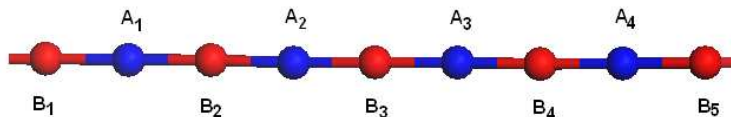

Figure 1: Lattice $\mathcal{L}_{su(2)}$ given by the superposition of two sublattices $\mathcal{A}_{su(2)}$ and $\mathcal{B}_{su(2)}$.

Each atom of this lattice, say an atom A_n of sublattice $\mathcal{A}_{su(2)}$, has two first nearest neighbors of B-type; that is B_n and B_{n+1}; for illustration see fig(1). The quantum states

---

[1]The acetylene is C_2H_2 with carbons in the sp^1 hybridization with *2* delocalized electrons. By chain we mean the C_mH_2 generalization with large integer m.

of the delocalized electrons of these atoms are described by the wave functions

$$A_n\left(x\right) \qquad = \int_{-\infty}^{+\infty} \frac{dk}{2\pi} e^{ikx} \tilde{A}_n\left(k\right) \qquad ,$$

$$B_n\left(x + v_i\right) = \int_{-\infty}^{+\infty} \frac{dk}{2\pi} e^{ik(x+v_i)} \tilde{B}_n\left(k\right) \quad ,$$

(2.1)

where v_0 and v_1 are the relative positions parameterizing the two first nearest neighbors. These $\mathbf{v}_i$'s satisfy the remarkable constraint relation

$$v_0 + v_1 = 0, \quad \rightarrow \quad v_0 = -v_1 = v \quad , \tag{2.2}$$

that turns out to have a nice group theoretic interpretation. More precisely, v_0 and v_1 are proportional to the weights of the isospinorial representations of $SU\left(2\right)$. By setting $v_1 = 2d\mu_1$ and $v_0 = 2d\mu_0$, it is clear that the constraint eq(2.2) is solved by the fundamental weights $\mu_0 = +\frac{1}{2}$ and $\mu_1 = -\frac{1}{2}$ of the $SU\left(2\right)$ doublet representation with dominant weight μ_0 and trace

$$2d\left(\mu_0 + \mu_1\right) = 2d\left(\tfrac{1}{2} - \tfrac{1}{2}\right) = 0 \quad . \tag{2.3}$$

the hamiltonian

By focusing on correlations between the first nearest neighbors, the tight binding hamiltonian reads as follows

$$\mathcal{H}_{SU(2)} \quad = -t\left(\mathcal{F}_v + \mathcal{F}_v^\dagger\right) - t\left(\mathcal{G}_v + \mathcal{G}_v^\dagger\right) \quad , \tag{2.4}$$

with t is the hop energy and where $\mathcal{F}_v$ and $\mathcal{G}_v$ are operators realized in terms of the electronic creation and annihilation ones $A_{x_m}^\pm$, $B_{x_m}^\pm$ as follows,

$$\mathcal{F}_v = \sum_{m\in\mathbb{Z}} A_{x_m}^- B_{x_m+v}^+ \quad , \quad \mathcal{F}_v^\dagger = \sum_{m\in\mathbb{Z}} A_{x_m}^+ B_{x_m+v}^- \quad ,$$

$$\mathcal{G}_v = \sum_{m\in\mathbb{Z}} A_{x_m}^- B_{x_m-v}^+ \quad , \quad \mathcal{G}_v^\dagger = \sum_{m\in\mathbb{Z}} A_{x_m}^+ B_{x_m-v}^- \quad . \tag{2.5}$$

Notice by the way that the operator $\mathcal{F}_v$ describes electronic hops from left to right while $\mathcal{G}_v$ describes hops from right to left. These two hops generate two kinds of symmetries that we want to comment through a set of remarkable properties that turn out to be also valid for the higher dimensional extensions to be considered in next sections.

property 1: the above hamiltonian $\mathcal{H}_{SU(2)}$ is an adequate approximation to describe the electronic properties of the poly-acetylene. But a more concise description requires

however taking into account the effects beyond the first nearest couplings. These correlations can be thought of as corrections described by operators of the form,

$$\mathcal{F}_{nv} = \sum_{m\in\mathbb{Z}} A^-_{x_m} B^+_{x_m+nv} \quad, \quad \mathcal{F}^\dagger_{nv} = \sum_{m\in\mathbb{Z}} A^+_{x_m} B^-_{x_m+nv} \quad,$$

$$\mathcal{G}_{nv} = \sum_{m\in\mathbb{Z}} A^-_{x_m} B^+_{x_m-nv} \quad, \quad \mathcal{G}^\dagger_{nv} = \sum_{m\in\mathbb{Z}} A^+_{x_m} B^-_{x_m-nv} \quad. \tag{2.6}$$

with $n \geq 2$ generating an infinite dimensional Lie algebra. It happens that the restriction to first nearest neighbors breaks this infinite dimensional symmetry down to a sub-symmetry to be identified later on; see *property 3*.

property 2: the structure of the operator $\mathcal{H}_{SU(2)}$ is very particular; it recalls basic features of complex geometry, supersymmetry and step operators of Lie algebras. For the links with complex geometry and supersymmetry, one has just to notice that given some holomorphic function $F(Z)$ with a complex variable Z that can be interpreted as a chiral superfield in 4D supersymmetry [13]; one may build two fundamental kinds of real quantities namely

$$|F(Z)|^2 \quad \text{or} \quad F(Z) + \bar{F}(\bar{Z}) \quad, \tag{2.7}$$

in a quite similar manner with the Kahler $K(Z, \bar{Z})$ and chiral superpotentials $W(Z)$ of 4D supersymmetric non linear sigma models. From this view, the hamiltonian $\mathcal{H}_{SU(2)}$ is of the second type as it follows by setting

$$F(Z) = -t(\mathcal{F}_v + \mathcal{G}_v), \tag{2.8}$$

this feature may be also viewed as the reason behind the non diagonal form of the hamiltonian.

property 3: the third feature that we want to give here concerns the relation between $\mathcal{H}_{SU(2)}$ and $SU(2)$ Lie algebra; as this result is also valid for higher dimensions and higher rank groups; let us discuss it with some details here; and give just results for higher dimensional lattices to be considered later on.

There are two types of links between $\mathcal{H}_{SU(2)}$ (2.4); and the underlying $SU(2)$ symmetry:

- the first link concerns the 1D lattice $\mathcal{L}_{su(2)}$ which , up to some details, is nothing but the weight lattice of the $SU(2)$ Lie algebra. This is an integral lattice generated by the fundamental weight μ_0; i.e

$$\mathcal{L}_{su(2)} = \{x_m = mv = 2dm\mu_0, \quad m \in \mathbb{Z}\}. \tag{2.9}$$

6

Notice that the sublattice $\mathcal{A}_{su(2)}$ and $\mathcal{B}_{su(2)}$ are related to the root lattice of $SU(2)$ as already noticed before eq(1.1); and the superposition is done up to μ_0 shifts. This property become clearer when we consider bigger groups like SU(3); see for instance eqs(3.3-3.5) to fix the ideas.

- the second link concerns the physics described by the hamiltonian $\mathcal{H}_{SU(2)}$. From Lie algebra view, this hamiltonian is a very special quantity given by the sum over step operators of some infinite dimensional Lie algebra containing the following isomorphic $SU_L(2)$ and $SU_R(2)$ copies as subalgebras

$$
\begin{aligned}
\left[\mathcal{F}_v, \mathcal{F}_v^\dagger\right] &= \mathcal{N} \\
\left[\mathcal{N}, \mathcal{F}_v\right] &= -2\mathcal{F}_v \\
\left[\mathcal{N}, \mathcal{F}_v^\dagger\right] &= +2\mathcal{F}_v
\end{aligned}
\tag{2.10}
$$

and

$$
\begin{aligned}
\left[\mathcal{G}_v, \mathcal{G}_v^\dagger\right] &= \mathcal{N}' \\
\left[\mathcal{N}', \mathcal{G}_v\right] &= -2\mathcal{G}_v \\
\left[\mathcal{N}', \mathcal{G}_v^\dagger\right] &= +2\mathcal{G}_v^\dagger
\end{aligned}
\tag{2.11}
$$

where

$$
\mathcal{N} = \sum_{m\in\mathbb{Z}} \left(A_{x_m}^+ A_{x_m}^- + B_{y_m}^- B_{y_m}^+\right)
$$

$$
\mathcal{N}' = \sum_{m\in\mathbb{Z}} \left(A_{x_m}^+ A_{x_m}^- + B_{y_m'}^- B_{y_m'}^+\right)
\tag{2.12}
$$

with $y_m = x_m + v$ and $y_m' = x_m - v$.

To derive these commutation relations, we need to perform 3 steps; first use the realization eqs(2.5); second use also the algebra of the fermionic operators $A_{x_m}^\pm$ and $B_{y_m}^\pm$ satisfying the usual anticommutation relations namely

$$
\begin{aligned}
\left\{A_{x_m}^-, A_{x_n}^+\right\} = \delta_{nm} &\quad, \quad \left\{A_{x_m}^\pm, A_{x_n}^\pm\right\} = 0 \quad, \\
\left\{B_{y_m}^-, B_{y_n}^+\right\} = \delta_{nm} &\quad, \quad \left\{B_{y_m}^\pm, B_{y_n}^\pm\right\} = 0 \quad,
\end{aligned}
\tag{2.13}
$$

and

$$
\begin{aligned}
\left\{A_{x_m}^-, B_{y_n}^\pm\right\} &= 0 \\
\left\{A_{x_m}^+, B_{y_n}^\pm\right\} &= 0
\end{aligned}
\tag{2.14}
$$

and finally use the following relations

$$
\begin{aligned}
\left[\mathcal{N}, A_{x_m}^+\right] = +A_{x_m}^+ &\quad, \quad \left[\mathcal{N}, A_{x_m}^-\right] = -A_{x_m}^- \\
\left[\mathcal{N}, B_{y_m}^+\right] = -B_{y_m}^+ &\quad, \quad \left[\mathcal{N}, B_{y_m}^-\right] = +B_{y_m}^-
\end{aligned}
\tag{2.15}
$$

that show, amongst others that, $\left(A_{\mathbf{x}_m}^+, B_{y_m}^+\right)$ and $\left(B_{y_m}^-, A_{y_m}^-\right)$ form $SU(2)$ doublets under charge operator $\mathcal{N}$ and similarly with $\mathcal{N}'$.

Performing the Fourier transform of $A_{x_m}^\pm$ and $B_{x_m+v_i}^\pm$ as given above, we can bring this hamiltonian to the non diagonal form $\mathcal{H}_{SU(2)} = \sum_k \mathcal{H}_k^{su_2}$ with

$$\mathcal{H}_k^{su_2} = \left(\tilde{A}_k^-, \tilde{B}_k^-\right) \begin{pmatrix} 0 & e^{i2kd\mu_0} + e^{i2kd\mu_1} \\ e^{-i2kd\mu_0} + e^{-i2kd\mu_1} & 0 \end{pmatrix} \begin{pmatrix} \tilde{A}_k^+ \\ \tilde{B}_k^+ \end{pmatrix} \quad (2.16)$$

The diagonalization of this hamiltonian leads to the dispersion energy relation,

$$E_{su(2)}^\pm (k) = \pm t\sqrt{2 + 2\cos(2kd)} \quad (2.17)$$

which is associated with the usual conducting band $(+)$ and the valence one $(-)$. These relations can be also put into the form $\pm 2t \cos(kd)$ from which we read that their zeros (Fermi energy) take place for the wave vectors $k_n = \pm\frac{\pi}{2d} \bmod \frac{2\pi}{d}$.

3   Graphene as a $SU(3)$ model

Graphene, a sheet of graphite, is a 2D organic material system with carbons in the sp^2 hybridization. This material, which is of great interest nowadays, is expected to play a central role in nanotechnology [12, 14]. The graphene lattice denoted here as $\mathcal{L}_{su(3)}$ is a $2D$ honeycomb made by the superposition of two triangular sublattices $\mathcal{A}_{su(3)}$ and $\mathcal{B}_{su(3)}$ as depicted in fig(2).
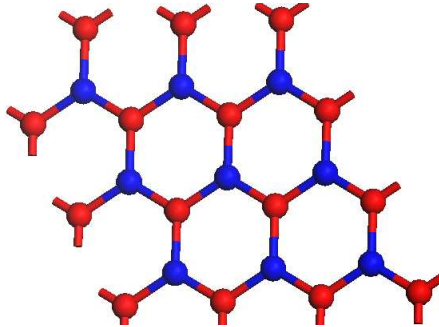

Figure 2: Sublattices $\mathcal{A}_{su(3)}$ (in blue) and $\mathcal{B}_{su(3)}$ (in red) of the honeycomb.

Each carbon atom, say $A_{\mathbf{r}_n}$ of the sublattice $\mathcal{A}_{su(3)}$, has 3 first nearest atom neighbors of $\mathcal{B}$-type namely $B_{\mathbf{r}_n+\mathbf{v}_0}, B_{\mathbf{r}_n+\mathbf{v}_1}, B_{\mathbf{r}_n+\mathbf{v}_2}$ where $\mathbf{v}_0$, $\mathbf{v}_1$, $\mathbf{v}_2$ are $2D$ vectors parameterizing

their relative positions with respect to $A_{\mathbf{r}_n}$. These vectors satisfy the following constraint relation

$$\mathbf{v}_0 + \mathbf{v}_1 + \mathbf{v}_2 = 0 \quad , \tag{3.1}$$

that should be compared with (2.2). Like in the previous $SU(2)$ case, this constraint equation turns out to have an interpretation in terms of $SU(3)$ group representations. Setting $\mathbf{v}_0 = \boldsymbol{\mu}_0 d$, $\mathbf{v}_1 = \boldsymbol{\mu}_1 d$, $\mathbf{v}_2 = \boldsymbol{\mu}_2 d$ where $d \simeq 1.42 \mathring{A}$ is the length of the carbon-carbon bond, we end with the identity $\boldsymbol{\mu}_0 + \boldsymbol{\mu}_1 + \boldsymbol{\mu}_2 = 0$ describing precisely the weight vectors of the $SU(3)$ fundamental representation. To fix the ideas on these weight vectors and the way they may be handled, we give below two comments.

(**1**) the explicit expressions of these weight vectors are given by

$$\boldsymbol{\mu}_1 = (\tfrac{\sqrt{2}}{2}, \tfrac{\sqrt{6}}{6}) \quad , \quad \boldsymbol{\mu}_2 = (-\tfrac{\sqrt{2}}{2}, \tfrac{\sqrt{6}}{6}) \quad , \quad \boldsymbol{\mu}_0 = -(0, \tfrac{\sqrt{6}}{3}) \quad . \tag{3.2}$$

These planar vectors have the same norm $\|\boldsymbol{\mu}_l\| = \tfrac{2}{3}$ and the same angle $(\boldsymbol{\mu}_i, \boldsymbol{\mu}_j) = \tfrac{2\pi}{3}$. They satisfy manifestly the identity $\boldsymbol{\mu}_0 + \boldsymbol{\mu}_1 + \boldsymbol{\mu}_2 = 0$ capturing the traceless property of the $SU(3)$ symmetry.

(**2**) the two generators of the sublattice $\mathcal{A}_{su(3)}$ are given by the two simple roots $\boldsymbol{\alpha}_1$ and $\boldsymbol{\alpha}_2$ of the Lie algebra of the $SU(3)$. These two simple roots may be expressed in, different, but equivalent ways; one way to do is in terms of the weight vectors $\boldsymbol{\mu}_0$, $\boldsymbol{\mu}_1$, $\boldsymbol{\mu}_2$ of the 3-dimensional representation of $SU(3)$,

$$\boldsymbol{\alpha}_1 = \boldsymbol{\mu}_1 - \boldsymbol{\mu}_2 \quad , \quad \boldsymbol{\alpha}_2 = \boldsymbol{\mu}_2 - \boldsymbol{\mu}_0. \tag{3.3}$$

Another way is in terms of the two fundamental weight vectors $\boldsymbol{\omega}_1$ and $\boldsymbol{\omega}_2$ of $SU(3)$ namely

$$\boldsymbol{\alpha}_1 = 2\boldsymbol{\omega}_1 - \boldsymbol{\omega}_2 \quad , \quad \boldsymbol{\alpha}_2 = 2\boldsymbol{\omega}_2 - \boldsymbol{\omega}_1$$

from which we learn

$$\begin{aligned} \boldsymbol{\mu}_1 &= \boldsymbol{\omega}_1 & , \\ \boldsymbol{\mu}_2 &= \boldsymbol{\omega}_2 - \boldsymbol{\omega}_1 & , \\ \boldsymbol{\mu}_0 &= -\boldsymbol{\omega}_2 & , \end{aligned} \tag{3.4}$$

and

$$\boldsymbol{\alpha}_i . \boldsymbol{\omega}_j = \delta_{ij}. \tag{3.5}$$

As such, sites $\mathbf{r}_\mathbf{n}^A$ and $\mathbf{r}_\mathbf{n}^B$ in the sublattice $\mathcal{A}_{su(3)}$ and $\mathcal{B}_{su(3)}$ read respectively as follows,

$$\mathbf{r}_\mathbf{n}^A = n_1 \boldsymbol{\alpha}_1 + n_2 \boldsymbol{\alpha}_2 \quad , \quad \mathbf{r}_\mathbf{n}^B = \mathbf{r}_\mathbf{n}^A + \mathbf{v}_l \quad , \tag{3.6}$$

where $\mathbf{n} = (n_1, n_2)$ with n_1 and n_2 integers; and where the 3 $\mathbf{v}_l$'s are as before. The tight binding hamiltonian $\mathcal{H}_{SU(3)}$ describing the electronic correlations restricted to the first nearest neighbors is given by

$$\mathcal{H}_{SU(3)} = -t \left(\mathcal{F}_{\mathbf{v}_1} + \mathcal{F}_{\mathbf{v}_1}^\dagger \right) - t \left(\mathcal{F}_{\mathbf{v}_2} + \mathcal{F}_{\mathbf{v}_2}^\dagger \right) - t \left(\mathcal{F}_{\mathbf{v}_0} + \mathcal{F}_{\mathbf{v}_0}^\dagger \right) \quad , \tag{3.7}$$

9

where t is the hop energy and where $\mathcal{F}_{\mathbf{v}_l}$ are step operators given by

$$\mathcal{F}_{\mathbf{v}_l} = \sum_m A^-_{\mathbf{r}_m} B^+_{\mathbf{r}_m + \mathbf{v}_l} \quad , \tag{3.8}$$

with $A^\pm_{\mathbf{r}_m}$ and $B^\pm_{\mathbf{r}_m + \mathbf{v}_l}$ satisfying the electronic anticommutation relations. Notice that the hamiltonian $\mathcal{H}_{SU(3)}$ and the 3 step operators $\mathcal{F}_{\mathbf{v}_l}$ are quite similar to those of the poly-acetylene chain namely $\mathcal{H}_{SU(2)}$ and the associated $\mathcal{F}_v$ and $\mathcal{G}_v$ operators. From these $\mathcal{F}_{\mathbf{v}_l}$'s, we can make 3 copies of triplets

$$\mathcal{F}_{\mathbf{v}_l}, \quad \mathcal{F}^\dagger_{\mathbf{v}_l}, \quad \mathcal{N}_{\mathbf{v}_l} = \left[\mathcal{F}_{\mathbf{v}_l}, \mathcal{F}^\dagger_{\mathbf{v}_l} \right] \quad , \tag{3.9}$$

each copy obeys an $SU(2)$ Lie algebra. Notice also that the $\mathcal{F}_{\mathbf{v}_l}$'s and $\mathcal{F}^\dagger_{\mathbf{v}_l}$'s are in fact particular operators of more general ones describing generic hops and generating an infinite dimensional symmetry.

Performing the Fourier transform of these field operators, we can put $\mathcal{H}_{SU(3)}$ into the form $\sum_{\mathbf{k}} \mathcal{H}^{su_3}_{\mathbf{k}}$ where $\mathbf{k} = (k_x, k_y)$ is the wave vector and where

$$\mathcal{H}^{su_3}_{\mathbf{k}} = \left(\tilde{A}^-_{\mathbf{k}}, \tilde{B}^-_{\mathbf{k}} \right) \begin{pmatrix} 0 & \varepsilon_{su_3}(\mathbf{k}) \\ \varepsilon_{su_3}(\mathbf{k}) & 0 \end{pmatrix} \begin{pmatrix} \tilde{A}^+_{\mathbf{k}} \\ \tilde{B}^+_{\mathbf{k}} \end{pmatrix} \tag{3.10}$$

with

$$\varepsilon_{su_3}(\mathbf{k}) = e^{id\mathbf{k}\cdot\boldsymbol{\mu}_0} + e^{id\mathbf{k}\cdot\boldsymbol{\mu}_1} + e^{id\mathbf{k}\cdot\boldsymbol{\mu}_2} \quad . \tag{3.11}$$

The diagonalization of this hamiltonian leads to the dispersion energy relations

$$E^\pm_{su(3)}(\mathbf{k}) = \pm t \sqrt{3 + 2\left[\cos(d\mathbf{k}\cdot\boldsymbol{\alpha}_1) + \cos(d\mathbf{k}\cdot\boldsymbol{\alpha}_2) + \cos(d\mathbf{k}\cdot\boldsymbol{\alpha}_3) \right]}, \tag{3.12}$$

with

$$\boldsymbol{\alpha}_1 = \boldsymbol{\mu}_1 - \boldsymbol{\mu}_2 \quad , \quad \boldsymbol{\alpha}_2 = \boldsymbol{\mu}_2 - \boldsymbol{\mu}_0 \quad , \quad \boldsymbol{\mu}_0 - \boldsymbol{\mu}_1 = \boldsymbol{\alpha}_3 = \boldsymbol{\alpha}_1 + \boldsymbol{\alpha}_2 \quad , \tag{3.13}$$

nothing but the positive roots of the $SU(3)$ symmetry. We will show below that the apparition of the roots in the dispersion energies is a general feature of tight binding model shared by the series of models classified by the Lie groups.

4 $SU(4)$ diamond model

In this model, the lattice $\mathcal{L}_{su(4)}$ is a 3-dimensional crystal made by two tetrahedral sublattices $\mathcal{A}_{su(4)}$ and $\mathcal{B}_{su(4)}$ whose superposition follows the same logic as in the poly-acetylene chain and the 2D honeycomb; see eqs(3.6) with $\mathbf{r}^A_{\mathbf{n}} = n_1 \boldsymbol{\alpha}_1 + n_2 \boldsymbol{\alpha}_2 + n_3 \boldsymbol{\alpha}_3$, the relative vectors $\mathbf{v}_l$ as in (4.1)-(4.3); and fig(3) for illustration.
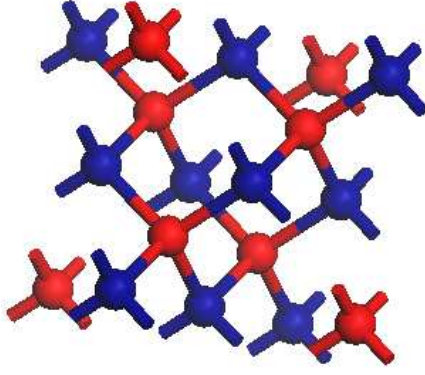
Figure 3: the lattice $\mathcal{L}_{su(4)}$ with sublattices $\mathcal{A}_{su(4)}$ (in blue) and $\mathcal{B}_{su(4)}$ (in red). Each atom has 4 first nearest neighbors forming a tetrahedron and 12 second nearest ones.

This physics describing electronic properties by using tight binding approach requires to go beyond the sp^1 and sp^2 hybridizations of the carbon atom considered in the two previous examples. Here, each atom, say of type $A_{\mathbf{r_n}}$ located at site $\mathbf{r_n}$, has 4 first nearest neighbors that can make 4 localized σ- bonds,

$$A_{\mathbf{r_n}} \rightarrow \begin{cases} B_{\mathbf{r_n}+\mathbf{v}_0} \\ B_{\mathbf{r_n}+\mathbf{v}_1} \\ B_{\mathbf{r_n}+\mathbf{v}_2} \\ B_{\mathbf{r_n}+\mathbf{v}_3} \end{cases} \tag{4.1}$$

So in case where atoms are carbons, there is no delocalized electrons of type π that can hop from a carbon to its closest neighbors; this is why carbon-diamond is an insulator. Nevertheless, in case where we have atoms that allows sp^3d^1 with delocalized electrons hoping to nearest neighboring tetrahedral sites; the tight binding approach applies as in previous case. To our understanding, this concerns in general material alloys with sp^3d^n hybridizations involving certain atoms of transition metals with delocalized d-electrons; for a related sp^3 tight-binding study concerning the calculation of the electronic and optical properties see [15].

On the other hand, as far as tight binding model on $3D$ diamond is concerned, one also may engineer simple toy models to describe quite similar physical properties as the electronic ones. Below, we develop a lattice model describing dynamical vacancies within the $3D$ crystal,

$$\mathcal{L}_{su(4)} = \mathcal{A}_{su(4)} \cup \mathcal{B}_{su(4)} \tag{4.2}$$

This is an ideal and simple toy model that is based on the two following heuristic hypothesizes:

11

- we assume that in the 3D lattice in its fundamental state has sites of the sublattice $\mathcal{A}_{su(4)}$ occupied by atoms; and the site of $\mathcal{B}_{su(4)}$ are vacancies; that is are unoccupied free sites.

- we also assume that under some external parameters, the atoms of $\mathcal{A}_{su(4)}$ leave their initial positions towards the free nearest neighbors in $\mathcal{B}_{su(4)}$; that A-atoms jump to $\mathcal{B}_{su(4)}$ and B-vacancies jump to $\mathcal{A}_{su(4)}$.

Actually one needs to specify other data; but let us forget about them by focusing on the ideal configuration; and look for the dispersion energies of the hop of atoms and vacancies in the *3D* lattice.

To that purpose, notice first that each site $\mathbf{r}_m$ in $\mathcal{L}_{su(4)}$ has *4* first nearest neighbors at $(\mathbf{r}_m + \mathbf{v}_i)$ as in eq(4.1) forming the vertices of a regular tetrahedron. These relative positions $\mathbf{v}_i$ are given by:

$$\begin{aligned}
\mathbf{v}_1 &= \tfrac{d}{\sqrt{3}}\left(-1,-1,+1\right) \quad, \quad \mathbf{v}_2 = \tfrac{d}{\sqrt{3}}\left(-1,+1,-1\right)\\
\mathbf{v}_3 &= \tfrac{d}{\sqrt{3}}\left(+1,-1,-1\right) \quad, \quad \mathbf{v}_0 = \tfrac{d}{\sqrt{3}}\left(+1,+1,+1\right)
\end{aligned} \tag{4.3}$$

and obey the constraint relation

$$\mathbf{v}_1 + \mathbf{v}_2 + \mathbf{v}_3 + \mathbf{v}_0 = 0$$

that should be compared with (2.2,3.1). Like in the previous $SU(2)$ and $SU(3)$ cases, this constraint equation has an interpretation in terms of $SU(4)$ group. Setting $\mathbf{v}_i = \tfrac{d}{\sqrt{3}}\boldsymbol{\mu}_i$, we end with

$$\boldsymbol{\mu}_0 + \boldsymbol{\mu}_1 + \boldsymbol{\mu}_2 + \boldsymbol{\mu}_3 = \mathbf{0} \quad, \tag{4.4}$$

showing that the $\boldsymbol{\mu}_i$'s are the weight vectors of the fundamental representation of SU(4) with dominant weight $\boldsymbol{\mu}_0$.

Let $A_{\mathbf{r}_m}$ and $B_{\mathbf{r}_m+\mathbf{v}_i}$ be the quantum states describing the particle at $\mathbf{r}_m$ and the vacancy at $\mathbf{r}_m + \mathbf{v}_i$ respectively. Let also $A^{\pm}_{\mathbf{r}_m}$ and $B^{\pm}_{\mathbf{r}_m+\mu_i}$ be the corresponding creation and annihilation operators. The hamiltonian describing the hop of the vacancy/particle to the first nearest neighbors is given by

$$\begin{aligned}
\mathcal{H}_{SU(4)} = \quad &-t\left(\mathcal{F}_{\mathbf{v}_1} + \mathcal{F}^{\dagger}_{\mathbf{v}_1}\right) - t\left(\mathcal{F}_{\mathbf{v}_2} + \mathcal{F}^{\dagger}_{\mathbf{v}_2}\right)\\
&-t\left(\mathcal{F}_{\mathbf{v}_3} + \mathcal{F}^{\dagger}_{\mathbf{v}_3}\right) - t\left(\mathcal{F}_{\mathbf{v}_0} + \mathcal{F}^{\dagger}_{\mathbf{v}_0}\right) \quad,
\end{aligned} \tag{4.5}$$

where the $\mathcal{F}_{\mathbf{v}_l}$'s are step operators given by

$$\mathcal{F}_{\mathbf{v}_l} = \sum_m A^{-}_{\mathbf{r}_m} B^{+}_{\mathbf{r}_m+\mathbf{v}_l} \quad. \tag{4.6}$$

12

By performing Fourier transforms of the $A^{\pm}_{\mathbf{r}_m}$, $B^{\pm}_{\mathbf{r}_m+\mu_i}$ field operators and following the same steps as in the SU(2) and SU(3) cases, we end with the remarkable form of the dispersion energies

$$E^{\pm}_{su_4}(\mathbf{k}) = \pm t \sqrt{4 + 2 \sum_{0 \leq i < j \leq 3} \cos\left(\frac{d}{\sqrt{3}}\mathbf{k}.\boldsymbol{\alpha}_{ij}\right)} \quad , \tag{4.7}$$

with $\mathbf{k} = (k_x, k_y, k_z)$ is the wave vector and where

$$\boldsymbol{\alpha}_{ij} = \boldsymbol{\mu}_i - \boldsymbol{\mu}_j \quad , \tag{4.8}$$

are exactly the *12* roots of the *SU*(4) group.

5 Octahedral $SO(6)$ model

The lattice $\mathcal{L}_{SO(6)}$, whose unit cell is given by the figure (4), is an other 3-dimensional crystal made by the superposition of two octahedral sublattices $\mathcal{A}_{SO(6)}$ and $\mathcal{B}_{SO(6)}$. Each atom $A_{\mathbf{r_n}}$ located at site $\mathbf{r_n}$ has *6* first nearest neighbors,

$$A_{\mathbf{r_n}} \rightarrow \begin{cases} B_{\mathbf{r_n}+\mathbf{v}_1} \\ B_{\mathbf{r_n}+\mathbf{v}_2} \\ B_{\mathbf{r_n}+\mathbf{v}_3} \\ B_{\mathbf{r_n}+\mathbf{v}_4} \\ B_{\mathbf{r_n}+\mathbf{v}_5} \\ B_{\mathbf{r_n}+\mathbf{v}_6} \end{cases} \tag{5.1}$$

Unlike the *SU*(4) model, each atom in the lattice $\mathcal{L}_{SO(6)}$ give rather *6* bonds as in fig(4); so this model might be used to describe the electronic properties of material alloys which have sp^3d^2 hybridization with delocalized d-electrons hoping to nearest neighboring octahedral sites.

Below, we will also use the toy model described in section 4; but now with the *3D* lattice $\mathcal{L}_{SO(6)}$. Sites of the sublattice $\mathcal{A}_{SO(6)}$ are occupied by atoms and those of the site $\mathcal{B}_{SO(6)}$ are free vacancies. We also assume that under external parameters, the atoms and vacancies of $\mathcal{L}_{SO(6)}$ leave their initial positions and move towards the first nearest neighbors.

To study the dynamical properties of this toy model, notice first that each site $\mathbf{r}_m$ in $\mathcal{L}_{SO(6)}$ has *6* first nearest neighbors at $(\mathbf{r}_m + \mathbf{v}_I)$ forming the vertices of an octahedron as shown on the fig(4) and eq(5.1). Like in previous models, the relative positions $\mathbf{v}_I$ obey the constraint relation

$$\mathbf{v}_1 + \mathbf{v}_2 + \mathbf{v}_3 + \mathbf{v}_4 + \mathbf{v}_5 + \mathbf{v}_6 = 0 \quad , \tag{5.2}$$
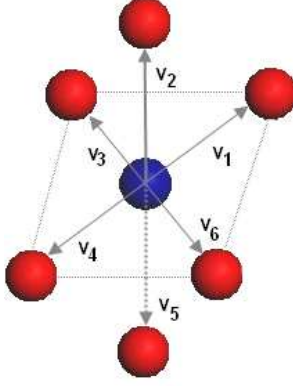
13

Figure 4: Each atom has *6* first nearest forming an octahedron.

having as well a group theoretic interpretation depending on the way it is solved. Strictly speaking, there are various ways to solve this constraint relation; but for the case at hand, it is solved as follows: First split the set of the *6* vectors into two subsets like,

$$
\mathbf{v}_I \quad = \quad \left\{ \begin{array}{l} v_i^+ = \mathbf{v}_i \\ v_i^- = \mathbf{v}_{3+i} \end{array} \right. \quad , \quad i = 1, 2, 3 \tag{5.3}
$$

so that the constraint relation (5.2) takes the form $\sum_i \left(v_i^+ + v_i^- \right)$. Then solve the vanishing condition by taking $v_i^- = -v_i^+$; this leads to the octahedron of fig(4). Moreover, setting $\mathbf{v}_I = d\boldsymbol{\mu}_I$ with factor d the atom-vacancy distance, one can check explicitly that the $\boldsymbol{\mu}_I$s are nothing but the weights of the $SO\left(6\right)$ vector representation. Recall that $SO\left(6\right)$ has rank *3* and dimension *15*; it also has 12 roots $\boldsymbol{\alpha}_{IJ}$, three of them denoted $\boldsymbol{\alpha}_i$ are simple; the $\boldsymbol{\alpha}_{IJ}$s are like $\pm \left(\boldsymbol{\mu}_i \pm \boldsymbol{\mu}_j \right)$ with $1 \leq i, j \leq 3$ and the simple ones are given by

$$
\boldsymbol{\alpha}_1 = \boldsymbol{\mu}_1 - \boldsymbol{\mu}_2, \quad \boldsymbol{\alpha}_2 = \boldsymbol{\mu}_2 - \boldsymbol{\mu}_3, \quad \boldsymbol{\alpha}_3 = \boldsymbol{\mu}_2 + \boldsymbol{\mu}_3. \tag{5.4}
$$

The tight binding hamiltonian $\mathcal{H}_{SO(6)}$ describing the hop of the vacancy/particle to the first nearest neighbors is given by,

$$
\begin{array}{rl}
\mathcal{H}_{SO(6)} = & -t \left(\mathcal{F}_{\mathbf{v}_1} + \mathcal{F}_{\mathbf{v}_1}^\dagger \right) - t \left(\mathcal{F}_{\mathbf{v}_2} + \mathcal{F}_{\mathbf{v}_2}^\dagger \right) - t \left(\mathcal{F}_{\mathbf{v}_3} + \mathcal{F}_{\mathbf{v}_3}^\dagger \right) \\
& -t \left(\mathcal{F}_{\mathbf{v}_4} + \mathcal{F}_{\mathbf{v}_4}^\dagger \right) - t \left(\mathcal{F}_{\mathbf{v}_5} + \mathcal{F}_{\mathbf{v}_5}^\dagger \right) - t \left(\mathcal{F}_{\mathbf{v}_6} + \mathcal{F}_{\mathbf{v}_6}^\dagger \right) \quad ,
\end{array} \tag{5.5}
$$

where the $\mathcal{F}_{\mathbf{v}_l}$'s are step operators given by $\sum_m A_{\mathbf{r}_m}^- B_{\mathbf{r}_m+\mathbf{v}_l}^+$. By performing Fourier transforms of the $A_{\mathbf{r}_m}^\pm$, $B_{\mathbf{r}_m+V_I}^\pm$ field operators and following the same steps as before, we end with the dispersion energy relations

$$
E_{so_6}^\pm \left(\mathbf{k} \right) = \pm t \sqrt{6 + 2 \sum_{0 \leq I < J \leq 6} \cos \left(d \, \mathbf{k}.\boldsymbol{\alpha}_{IJ} \right)} \quad , \tag{5.6}
$$

with $\mathbf{k} = (k_x, k_y, k_z)$ is the wave vector and $\boldsymbol{\alpha}_{IJ}$ the roots of $SO\left(6\right)$.

14

6 Conclusion and comments

In the present paper, we have used tight binding approach and continuous group representation methods to engineer a series of lattice QFT models classified by ADE Lie groups. These lattice models include the electronic properties of the *1D* poly-acetylene chain and *2D* graphene, but also dynamical properties of the vacancies in lattice models such as the $SU(4)$ diamond and the $SO(6)$ octahedron considered in this study. As a remarkable fact following this set of models is that the dispersion energies, restricted to first nearest neighbors couplings, are completely characterized by the roots of the Lie algebras underlying the crystals. The lattice QFT models considered here are associated with low rank groups as required by condensed matter systems with real dimension at most *3*. If relaxing this condition to include higher dimensions; the results obtained in this paper extend naturally to the $SU(N)$ and $SO(N)$ series. We end this study by first noting that there still is an interesting issue that might have interpretation in condensed matter systems; it concerns the models based on $SO(5)$ and G_2 groups having rank *2* and associated with non simply laced Lie algebras; atoms living at sites of the lattice $\mathcal{L}_{SO(5)}$, whose *5* first nearest neighbors form a vector representation of a hidden $SO(5)$ symmetry, allows five bonds and would corresponds to the $sp^3 d^1$ hybridization as shown of fig(5).
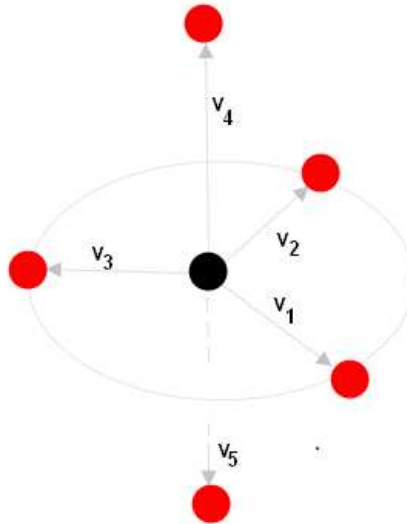

Figure 5: *bonds in the dsp^3 hybridization with the 5 first nearest neighbors form a vector representation of a hidden $SO(5)$ symmetry.*

Notice also that lattice model based on *4D* hyperdiamond has $SU(5)$ symmetry; it has been related in [6, 16] with lattice QCD; see also [17]-[19],[7].

References

[1] P.R Wallace, Phys Rev 71, (1947), 622,

[2] G.V. Semenoff, Phys. Rev. Lett. 53, 2449 (1984),

[3] K. S Novoselov et al, Science 306 (2004) 666,

[4] A.H.Castro-Neto et al. Rev. Mod. Phys.81, 109 (2009),

[5] L.B Drissi, E.H Saidi, M.Bousmina, Nucl Phys B, Vol 829, p.523-533, arXiv:1106.5222,

[6] L.B Drissi, E.H Saidi, M.Bousmina, *4D graphene*, Phys Rev D (2011), in press, arXiv:1106.5222

[7] L.B Drissi, H. Mhamdi, E.H Saidi, *Anomalous Quantum Hall Effect of 4D Graphene in Background Fields*, arXiv:1106.5578,

[8] M.S. Dresselhaus, G. Dresselhaus, A. Jorio, *Group Theory. Applications to the Physics of Condensed Matter*, Springer, Berlin, 2008,

[9] Brian C. Hall Lie Groups, *Lie Algebras, and Representations: An Elementary Introduction,* Springer, 2003. ISBN 0-387-40122-9,

[10] P. Goddard and D. Olive, *Kac-Moody and Virasoro algebras in relation to quantum physics,* Int. Journ. of Mod. Phys. A 1, 303-414, 1986,

[11] R. Ahl Laamara, M. Ait Ben Haddou, A Belhaj, L.B Drissi, E.H Saidi, Nucl.Phys. B702 (2004) 163-188,

[12] Gunn Kim, Yeonju Kim, Jisoon Ihm, Chemical Physics Letters v. 415, p.279 (2005), arXiv:cond-mat/0506748,

[13] J. Wess, J. Bagger, *Supersymmetry and Supergravity*, Princeton University Press, Prince- ton, 1983,

[14] A. K. Geim, Graphene: *Status and Prospects*, Science 19, Vol. 324. no. 5934, pp. 1530 - 1534, (2009),

[15] S. Schulz, S. Schumacher, G. Czycholl, Phys. Rev. B73, 245327 (2006), arXiv:0802.2436,

[16] Lalla Btissam Drissi, El Hassan Saidi, *On Dirac Zero Modes in Hyperdiamond Model*, arXiv:1103.1316, Under consideration in Phys Rev D.

[17] Michael Creutz, *Four dimensional graphene and chiral fermions*, JHEP0804:017,2008, arXiv:0712.1201,

[18] Taro Kimura, Tatsuhiro Misumi, Prog.Theor.Phys.123: 63-78, (2010), arXiv:0907.3774,

[19] T. Kimura and T. Misumi, Prog.Theor.Phys.124: 415-432, (2010), arXiv:0907.1371,

[20] Michael Creutz, Tatsuhiro Misumi, *Classification of Minimally Doubled Fermions*, Phys.Rev.D82:074502,2010, arXiv:1007.3328,